Dalton Transactions

Using lead chalcogenide nanocrystals as spin mixers: a perspective on near-infrared-to-visible upconversion

Journal:	*Dalton Transactions*
Manuscript ID	DT-PER-02-2018-000419.R1
Article Type:	Perspective
Date Submitted by the Author:	22-Feb-2018
Complete List of Authors:	Nienhaus, Lea; Massachusetts Institute of Technology, Chemistry Wu, Mengfei; Massachusetts Institute of Technology, Electrical Engineering and Computer Science Bulovic, Vladimir; Massachusetts Institute of Technology, Electrical Engineering and Computer Science Baldo, Marc; Massachusetts Institute of Technology, Electrical Engineering and Computer Science Bawendi, Moungi; MIT, Chemistry

Using lead chalcogenide nanocrystals as spin mixers: a perspective on near-infrared-to-visible upconversion

Lea Nienhaus†, Mengfei Wu†, Vladimir Bulović, Marc A. Baldo* and Moungi G. Bawendi*

† *These authors contributed equally*
Massachusetts Institute of Technology, Cambridge, MA, 02139, USA
* *E-mail: baldo@mit.edu and mgb@mit.edu*

ABSTRACT

The process of upconversion leads to emission of photons higher in energy than the incident photons. Near-infrared-to-visible upconversion, in particular, shows promise in sub-bandgap sensitization of silicon and other optoelectronic materials, resulting in potential applications ranging from photovoltaics that exceed the Shockley-Queisser limit, to infrared biological imaging. A feasible mechanism for near-infrared-to-visible upconversion is triplet-triplet annihilation (TTA) sensitized by colloidal nanocrystals (NCs). Here, the long lifetime of spin-triplet excitons in the organic materials that undergo TTA makes upconversion possible under incoherent excitation at relatively low photon fluxes. Since this process relies on optically inactive triplet states, semiconductor NCs are utilized as efficient spin mixers, absorbing the incident light and sensitizing the triplet states of the TTA material. The state-of-the-art system uses rubrene with a triplet energy of 1.14 eV as the TTA medium, and thus allows upconversion of light with photon energies above ~1.1 eV. In this perspective, we review the field of lead sulfide (PbS) NC-sensitized near-infrared-to-visible upconversion, discuss solution-based upconversion, and highlight progress made on solid-state upconversion devices.

TOC

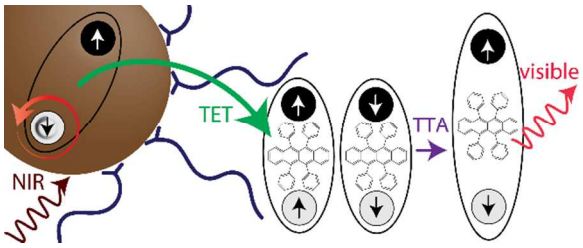

This perspective highlights recent advancements in the field of PbS NC-sensitized near-infrared-to-visible upconversion based on triplet-triplet annihilation in rubrene.

PERSONAL

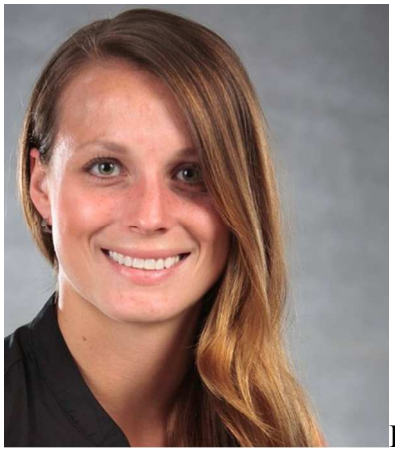 Lea Nienhaus was awarded a B.Sc. from the Universität Ulm, Germany in 2010. She then moved to the University of Illinois at Urbana-Champaign to pursue a PhD in Chemistry, working with Dr. Martin Gruebele on nanometer-resolved imaging of optical absorption in nanomaterials by scanning tunneling microscopy. After obtaining her PhD in 2015 she joined the Bawendi Lab at MIT, where she is currently working as a postdoctoral researcher. Her work focuses on unraveling the energy transfer dynamics in hybrid inorganic-organic upconverting devices and investigating the charge-carrier dynamics in emerging perovskite materials.

 Mengfei Wu joined MIT as a graduate student in 2013, pursuing a Ph.D. in Electrical Engineering, after receiving B.A. and M.Eng from the University of Cambridge, UK in 2012. Her graduate research focuses on the design, fabrication, and characterization of solid-state thin-film upconversion devices based on colloidal nanocrystals and organic molecules. She is interested in the integration of upconversion devices with optoelectronic and photonic systems.

 Vladimir Bulović is the Associate Dean for Innovation in MIT's School of Engineering, overseeing a broad portfolio of efforts that support innovation and entrepreneurship. He is a Professor of Electrical Engineering leading the Organic and Nanostructured Electronics laboratory. He holds over 100 U.S. patents in areas of light emitting diodes, lasers, photovoltaics, photodetectors, chemical sensors, programmable memories, and micro-electro machines. The three start-up companies (Ubiquitous Energy, Inc., Kateeva, Inc. QD Vision, Inc) that Bulović and his students co-founded jointly employ over 450 people, and generate technology that has reached millions.

 Marc Baldo is the Director of the Research Laboratory of Electronics at MIT, and Director of the Center for Excitonics, an Energy Frontier Research Center sponsored by the US Department of Energy. He received his B.Eng. from the University of Sydney in 1995 and Ph.D. in Electrical Engineering from Princeton in 2001. His research studies the excitonic properties of organic materials and nano materials. Awards include the Jan Rajchman Prize in 2013 from the Society for Information Display.

 Moungi Bawendi holds the Lester Wolfe Chair in Chemistry at MIT. He received his AB from Harvard University in 1982, followed by a PhD in Chemistry from the University of Chicago. His postdoctoral research took place at Bell Laboratories with Dr. Louis Brus. In 1990 he joined the faculty at MIT, and has since led an interdisciplinary research program aimed at advancing both fundamental understanding and technological applications of nanomaterials. He is a Fellow of the American Academy of Arts and Sciences, the American Association for the Advancement of Science, and a member of the National Academy of Sciences.

INTRODUCTION

Silicon is ubiquitous in optoelectronic devices, ranging from solar cells to imaging arrays. Despite its versatility, silicon (like all other semiconductors) cannot respond to sub-bandgap photons. Sensitization of silicon for sub-bandgap photons is an attractive possibility, potentially boosting the power conversion efficiency of single-junction solar cells beyond the Shockley-Queisser limit,[1,2] and enabling inexpensive silicon-based devices for infrared detection and imaging.[3] Other semiconducting solar materials such as lead halide perovskites, which have recently shown rapid progress in photovoltaics, will also likely benefit from sub-bandgap sensitization, given their relatively large bandgaps.[4–7] Photon upconversion, a process that converts two or more low-energy photons into a single higher-energy photon, could be utilized in such sub-bandgap sensitization. For example, two or more near-infrared (NIR) photons below the bandgap of silicon could combine into a single visible photon above the bandgap, thus trigger a response in a silicon-based device. Besides sub-bandgap sensitization for photovoltaic and detection applications,[2] NIR-to-visible upconversion also has potential applications in biological imaging,[8–10] 3-dimensional displays,[11,12] and photocatalysis.[13,14]

There are two major schemes of NIR-to-visible upconversion apart from second harmonic generation in nonlinear crystals.[15] One is based on luminescent lanthanide ions, relying on their

long-lived and ladder-like electronic states.[13,16–19] The other employs organic molecules, taking advantage of long-lived optically inactive or "dark" triplet states.[20–24] In the following, we will focus on the molecular-based upconversion process, in which two NIR photons are combined via diffusion-mediated triplet-triplet annihilation (TTA) in organic semiconductors, known as annihilators. In comparison to lanthanide-based upconverters, which typically require a high incident photon flux, the diffusion-mediated TTA process has the benefit of occurring efficiently at (sub-)solar fluxes.[22] In TTA, two adjacent spin-triplet excitons interact to obtain one higher-energy spin-singlet exciton. As triplet states are spin-forbidden to couple radiatively to the ground state, they cannot be directly excited optically and require a triplet sensitizer. The triplet sensitizer absorbs the light into a singlet state and converts the energy into a triplet state by an allowed process, such as intersystem crossing (ISC) in metal-organic complexes[20,25] or exchange-interactions in semiconductor nanocrystals (NCs).[21–23]

PbS NANOCRYSTALS AS TRIPLET SENSITIZERS

Infrared PbS colloidal NCs have been shown to be efficient triplet sensitizers due to their unique photophysical properties,[21,22] and have the advantage of a simple synthetic tunability of their optical properties and low-cost scalability.[26] Unlike ISC in metal-organic complexes, which results in an energy loss of hundreds of meV due to a high exchange splitting of the singlet and triplet states in the sensitizer,[27] NCs are able to interconvert an optically "bright" singlet state into a "dark" triplet state without significant energy loss, a result of their electronic fine structure.[28] Due to strong spin-orbit coupling in the NC, the exchange interaction between the singlet and triplet states is only on the order of 1-25 meV.[26] As a result, the band-edge exciton undergoes rapid spin dephasing, and has both singlet and triplet character at room temperature.[28] The optically excited infrared "triplet" exciton on the NC can then undergo a spin-allowed energy transfer into the triplet state of the annihilator, for instance rubrene, as the spin state is maintained. Fig. 1 illustrates the upconversion process in solid-state devices: the PbS NC is optically excited, and undergoes energy transfer into the triplet state of rubrene. Singlets are obtained via TTA, and are rapidly harvested by Förster resonance energy transfer (FRET) to the emissive dopant dibenzotetraphenylperiflanthene (DBP).[29] This additional step is required in solid-state devices due to the otherwise low fluorescence quantum yield (QY) of rubrene film, resulting from singlet fission.[21]

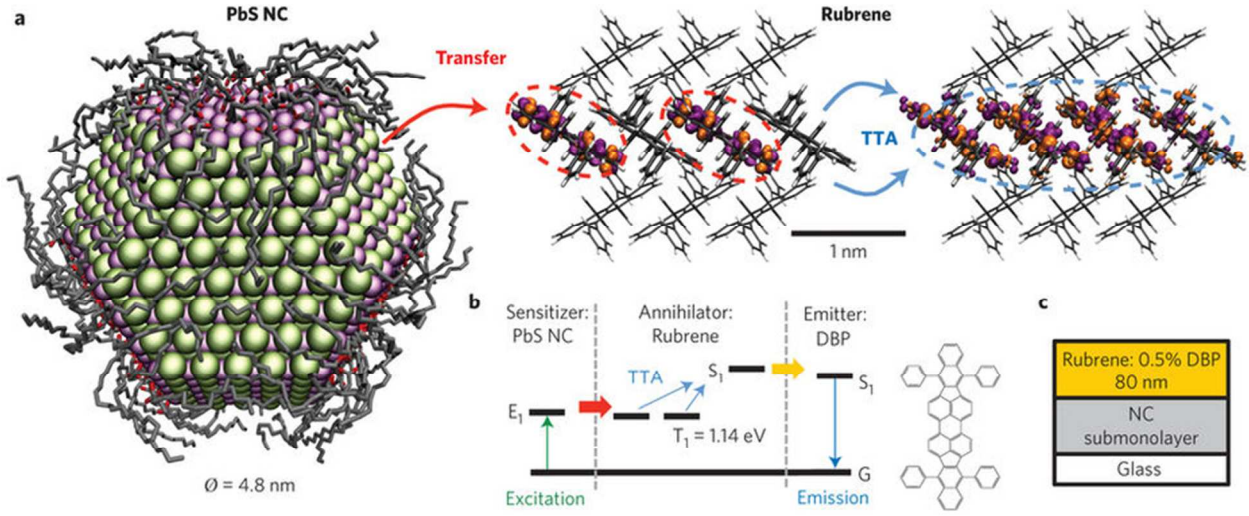

Figure 1: Schematic of the NC-sensitzed TTA based upconversion process. (a) PbS NCs are optically excited and transfer energy to the triplet state of the annihilator rubrene. The localized triplet excitons are circled in red, and if two triplet excitons collide via diffusion, a higher-energy singlet exciton can be formed. The resulting delocalized singlet exciton is cirlced in blue. (b) Schematic energy diagram. (c) Solid-state device structure. Reprinted from Ref. 21.

TRIPLET ENERGY TRANSFER MECHANISMS

The triplet energy transfer (TET) from the PbS sensitizer to the annihilator is commonly thought to occur via an exchange-mediated energy transfer mechanism, i.e. Dexter transfer.[30] Dexter transfer is based on a direct wavefunction overlap of the donor and acceptor states, resulting in electronic coupling between the two states. During energy transfer, a concerted electron swap occurs between the respective ground and excited states, while maintaining the spin of the initial state. As the wavefunction decays exponentially with distance, the electronic coupling and therefore also the rate of TET (k_{TET}) are expected to be exponentially dependent on the donor-acceptor spacing r

$$k_{TET} \sim \exp\left(\frac{-2r}{L}\right), \quad (1)$$

where L is the characteristic length of the energy transfer.

Dexter is a short-range energy transfer mechanism due to the requirement of a wavefunction overlap. Therefore, a 10 Å maximum length scale for the donor-acceptor spacing is usually expected for this energy transfer mechanism.[31] In exchange-mediated energy transfer processes involving NCs, larger donor-acceptor separations have been observed, while maintaining efficient energy transfer.[21,32,33] The underlying cause of this effect has not been unambiguously identified. However, it has been speculated to be a result of a large wavefunction leakage in PbS

NCs,[34] or caused by incomplete surface ligand coverage, which results in a reduced donor-acceptor spacing.[35]

In our solid-state devices, we infer a Dexter mechanism for TET from the NCs to the annihilator rubrene.[32] To investigate the TET phenomenon further, we perform ligand exchange to modulate the donor-acceptor spacing, which is expected to translate into an exponential dependence of k_{TET} on the ligand length. However, we find through time-resolved photoluminescence (PL) measurements that the rate of energy transfer plateaus for relatively short ligands (Fig. 2b), which we attribute to reduced electronic coupling between the donor and acceptor due to an increase in the effective dielectric constant of the NC thin film, calculated from an effective medium approximation based on the Bruggeman model (Fig. 2a).[36] After accounting for the effects of dielectric screening, we are able to recover the inverse exponential dependence of the rate of energy transfer on the ligand length as predicted from the Dexter exchange mechanism (Fig. 2c).[32]

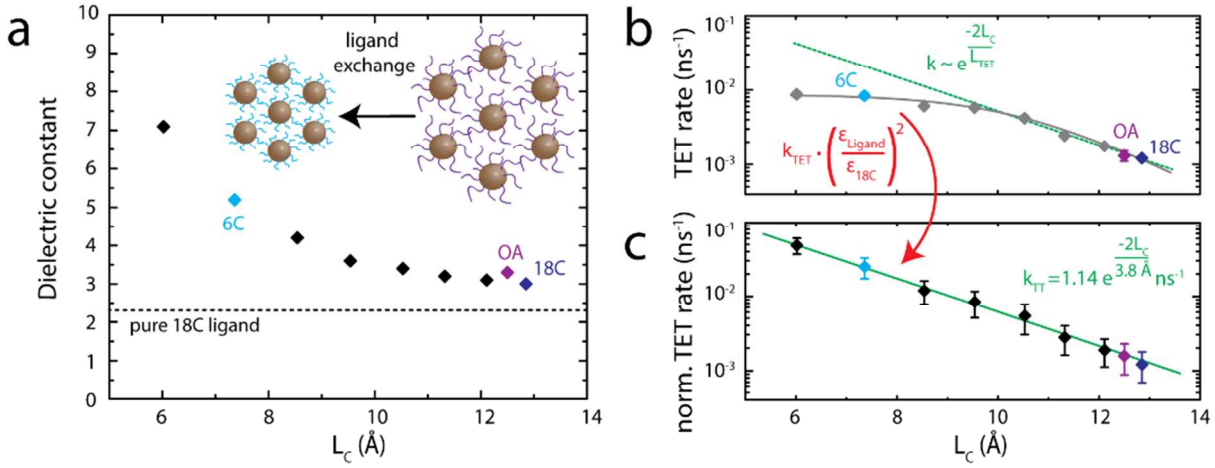

Figure 1: (a) Dielectric constant of the PbS NC film as a function of the ligand length based on an effective medium approximation. (b) The extracted k_{TET} as a function of the ligand length highlights the rate saturation for ligands shorter than ca. 10 Å. (c) k_{TET} corrected by the effective dielectric constant, which recovers the expected exponential trend of k_{TET} with ligand length. Reprinted with permission from Ref. 32. Copyright 2017 American Chemical Society.

An alternative TET mechanism based on delayed triplet generation, which is inconsistent with direct concerted Dexter transfer observed by our group[32] and Tang and co-workers,[22,23,37,38] has been proposed by Garakyaraghi *et al.*[39] for a carboxylic acid derivative of TIPS-pentacene (TPn) surface-bound on PbS NC. Here, the triplet is generated by charge separation at the PbS-TPn interface first, followed by time-delayed charge recombination. Fig. 3 highlights the relevant energy levels of the PbS NC and the structure and energy levels of the surface-bound TPn (left). The proposed delayed triplet generation on TPn is thought to be the result of formation of a

charge-separated state at the interface due to a single-charge transfer process: an electron from the TPn ground state fills the empty valence band state of the exciton on the PbS NC. This results in a TPn radical cation, and a negatively charged PbS NC: $TPn^{+\bullet}$-PbS(e^-). From this long-lived (τ = 6 ns) charge-transfer intermediate, the surface-bound triplet state ^{3}TPn-PbS is created following charge recombination (right).

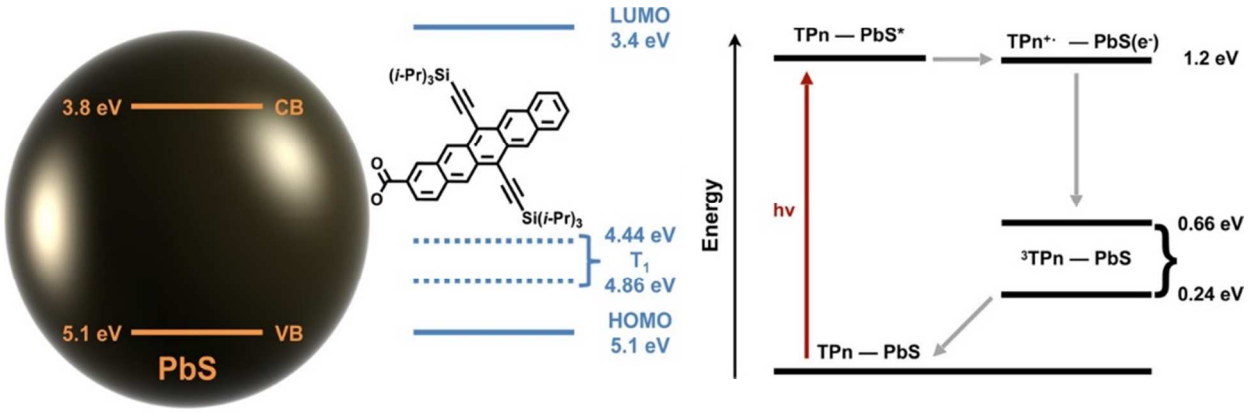

Figure 2: (Left) Schematic of the relevant energy levels in the PbS NC and the surface-bound TPn (structure shown). (Right) Energy level diagram and proposed pathway of the delayed triplet generation observed. PbS is selectively excited (TPn-PbS) and forms a charge-separated state at the interface: $TPn^{+\bullet}$-PbS(e^-). Delayed charge recombination results in the surface-bound triplet state ^{3}TPn-PbS, followed by relaxation of the triplet to the ground state. Adapted from Ref. 39. Copyright 2017 American Chemical Society.*

TRANSMITTER LIGANDS

NC quantum dots are surrounded by a layer of surface-passivating ligands.[40,41] These are required to maintain a high photoluminescence quantum yield (PLQY) of the NCs by passivating dangling bonds and therefore reducing non-radiative recombination centers. However, they pose a direct hurdle for the upconversion process, as they act as a spacer between the PbS donor and the organic annihilator, the acceptor of the triplet exciton via Dexter transfer. As mentioned earlier, this exchange-mediated energy transfer process is exponentially dependent on the donor-acceptor spacing.[30,32] To address this issue and increase the upconversion QY, Tang and co-workers have developed mediating transmitter ligands which facilitate the requirement of the wavefunction overlap between the donor and acceptor by creating an energy cascade from the NC to the annihilator.[22,38] These surface-bound transmitter ligands harvest the triplet excitons from the PbS NC via TET, and in turn undergo TET to nearby annihilator molecules. The main requirement for the feasibility of a molecule to act as a transmitter ligand is a triplet energy which lies between the triplet energy of the PbS donor and that of the organic annihilator.

However, there are additional factors which need to be taken into consideration: 1) the anchoring transmitter ligands need to bind tightly to the surface, while preserving the excitonic nature of the excited state and inhibiting single charge transfer (e.g. carboxylic and phosophonic acids). 2) The transmitter ligand must be chemically stable; upon excitation following the TET process it cannot undergo chemical reactions, such as Diels-Alder reactions.[42] Polyacene-based ligands with electron-withdrawing substituents show superior performance to their native counterparts. 3) High QYs, as this points to few alternative non-radiative recombination pathways in the transmitter ligand which could potentially outcompete the desire TET process. 4) To avoid detrimental triplet exciton quenching or TTA occurring between adjacent ligands, it is beneficial for the transmitter ligands to have rigid, bulky side groups to minimize unwanted intermolecular coupling. For the PbS/rubrene system described here, the transmitter ligands 5-carboxytetracene (5-CT) and 4-(tetracen-5-yl)benzoic acid (CPT) have shown success in improving the upconversion QY 37-fold and 81-fold, respectively, when compared to the neat PbS/rubrene system.[22,38,43]

PASSIVATING SHELLS TO INCREASE TRANSFER EFFCIENCY

One of the main difficulties in obtaining a high efficiency of TET, even after the requirements of a short donor-acceptor spacing and a high electronic coupling are met, is reducing the rate of charge transfer at the interface in favor of the preferred bound exciton transfer. It is also important to ensure that the TET process outcompetes alternative non-radiative recombination pathways. Using a wide bandgap semiconductor (e.g. cadmium sulfide CdS) as the shell material to obtain core-shell nanostructures has been shown to 1) increase the PLQY of PbS NCs by passivating the surface traps states arising from dangling bonds[44,45] and 2) suppress charge transfer.[37] However, thick CdS shells on PbS NCs add an additional tunneling barrier and result in a delocalized electron and a core-localized hole due to the expected quasi-type II band structure. Fig. 4a shows the absorption and emission spectra of the PbS/CdS core-shell NCs, highlighting a similar core size based on the location of the excitonic feature. Mahboub *et al.*[22] have been able to show an exponential dependence of the upconversion QY on the CdS shell thickness, as expected from a Dexter-type TET (Fig. 4b). The empirical damping coefficient of 3.4 $Å^{-1}$ is significantly higher than the damping coefficient of 0.52 $Å^{-1}$ observed in solid-state devices based on PbS core-only NCs.[32] This points to a much higher tunneling barrier through

the inorganic shell *vs*. the organic ligand shell, which can likely be attributed to a change in the electronic coupling between the donor and acceptor resulting from the different dielectric constants of the inorganic *vs.* organic ligand shell materials.[30]

As a result, there is a tradeoff between improved passivation and an increased tunneling barrier with respect to the ideal shell thickness: As the thickness of the passivating layer increases, the upconversion QY will increase due to an improved surface passivation, but the "high tunneling barrier" shell will reduce the tunneling rate with increasing thickness. Indeed, for the PbS/CdS sample in Ref. 22, a *ca.* 0.1 nm shell thickness (estimate based on the empirical equation by Moreels *et al.*[46]) shows the highest upconversion QY, as seen in Fig. 4c.

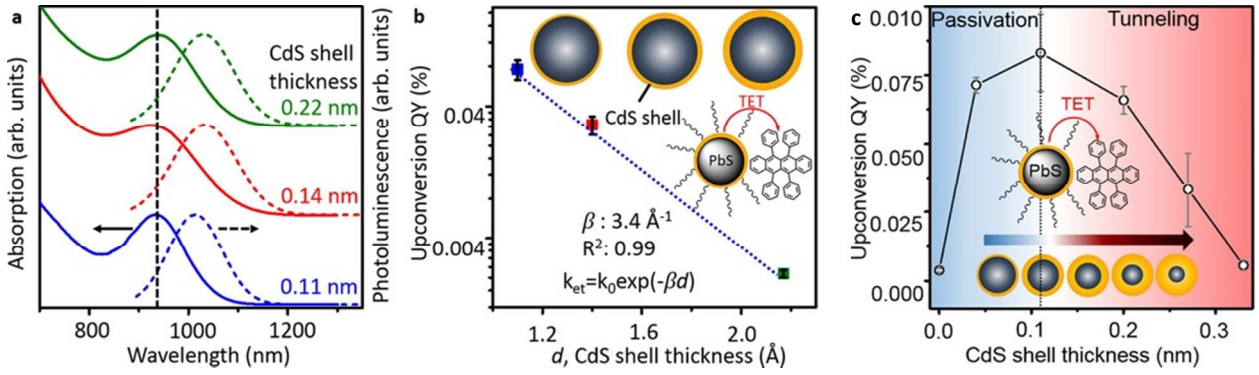

Figure 3: (a) Absorption (solid) and emission (dashed) spectra of the PbS/CdS core-shell quantum dots. The shell thickness is estimated based on the empirical equation by Moreels considering the original NC size and the shift in the absorption following shell growth by cation exchange. (b) Upconversion QY as a function of the shell thickness. (c) The upconversion QY first rises with increasing CdS shell thickness due to improved passivation, and then begins to fall with further increases in shell thickness due to the increased tunneling barrier caused by the CdS shell. Adapted with permission from Ref. 22. Copyright 2016 American Chemical Society.

SOLID-STATE UPCONVERSION DEVICES

To fabricate a solid-state upconversion device, we first deposit a thin layer of PbS NCs on glass by spin casting, and then thermally evaporate an 80nm-thick film of rubrene doped with DBP at 0.5 vol%.[21] The DBP dopant molecules, which have a high fluorescence QY, accept the energy from the singlets generated by TTA in rubrene through FRET and subsequently relax to emit visible light. The introduction of DBP boosts the PLQY of rubrene thin film by nearly twenty times while red shifting its PL from $\lambda = 570$ nm to $\lambda = 610$ nm. Thanks to the minimal energy loss in triplet sensitization by the NCs, we demonstrate TTA-based upconversion from excitation beyond $\lambda = 1$ μm to emission at $\lambda = 610$ nm in the solid state.[21] When excited at $\lambda = 808$ nm, (1.2±0.2)% of the excitons created in the sensitizer lead to the formation of higher-energy

emissive excitons in the annihilator.[21] We show that upconversion becomes efficient at an incident power density of 12 W/cm^2. Since the NC film in these devices is mostly submonolayer, which we estimate to absorb about 0.1% of the incident excitation photons, the threshold intensity is on the order of 12 mW/cm^2 *absorbed* in the NC film, similar to unconcentrated sunlight in terms of photon flux. This highlights the feasibility of utilization of TTA-based upconversion in photovoltaics and other low-intensity applications, provided that the absorption is near unity.

However, we find that in the above bilayer structure, the NC film has to be kept as thin as one or two monolayers to maximize the upconverted emission. While absorption is higher than that of a submonolayer, the film does not absorb more than 0.5% of the incident infrared light. The limitation on the NC thickness is likely due to short diffusion length of excitons in the NC film – excitons have to be photo-generated close to the hetero-interface in order to transfer their energy to rubrene – and increased reabsorption of visible emission with a thicker NC film. Morphology might also play a part. We observe that crystallization of rubrene becomes more prominent with the presence of an underlying NC layer, and the thicker the NC film, the faster the crystallization. Such a change in morphology likely reduces the interaction between the NCs and rubrene, and thus lowers the upconversion efficiency.

To increase the infrared absorption, we enhance the optical field intensity in the NC film through interference effects. We achieve so by adding an optical spacer layer and a silver back reflector to the original bilayer (Fig. 5a, 5b).[47] By tuning the thickness of the spacer layer made of AlQ_3, we maximize the field intensity in the NC layer, thus achieving a five-fold boost in the infrared absorption and an-order-of-magnitude increase in the upconverted emission at λ = 610 nm when excited at λ = 980 nm, as shown in Fig. 5c. The device attains maximum efficiency at an *incident* power density of 1.1 W/cm^2,[47] an order of magnitude lower than our first report,[21] and two orders of magnitude lower than the alternative solid-state upconversion system based on luminescent lanthanide ions.[48] With increased infrared absorption and enhanced upconverted emission, we are able to measure the upconversion QY more accurately, updating the device efficiency to (1.6±0.2)% of absorbed infrared photons contributing to higher-energy singlet excitons when pumped at λ = 980 nm,[47] compared to (0.5±0.1)% measured earlier for devices with NCs of the same energy excited at λ = 808 nm.[21] This work highlights the usefulness of optical management in solid-state upconversion devices.

To further improve the device efficiency, we increase the rate of triplet energy transfer from the NCs to rubrene by shortening the organic ligands passivating the surface of the NCs. By adopting a short ligand consisting of 6 carbon atoms instead of the usual 18 in the native oleic acid, on NCs of slightly higher energy, and a device structure with interference enhancement, we achieve a record solid-state upconversion efficiency, turning (7±1)% of absorbed photons into higher-energy emissive states when pumped at λ = 808 nm.[32]

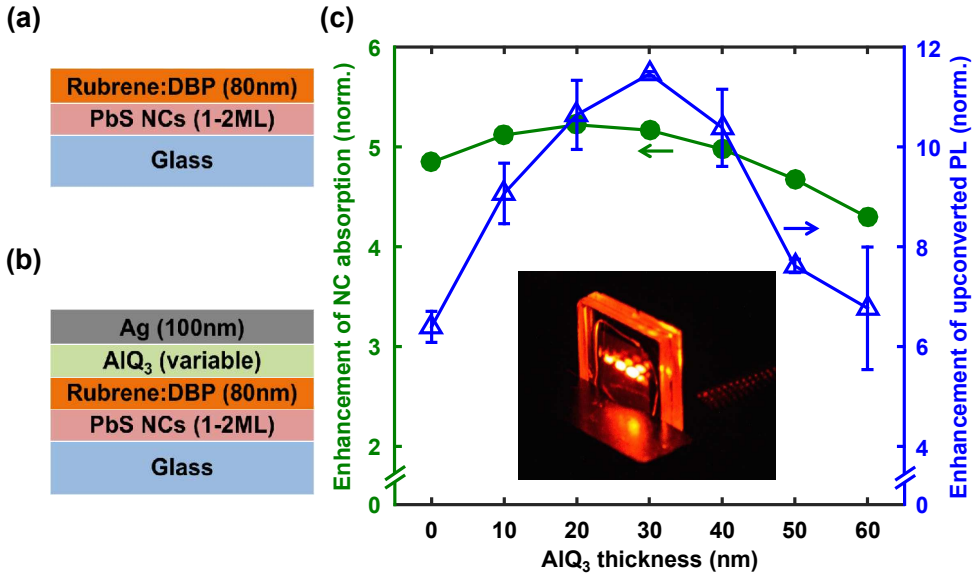

Figure 4: (a) Bilayer and (b) interference-enhanced device structure for solid-state upconversion devices. ML: monolayer. (c) Enhancement of NC absorption at λ = 980 nm (left y-axis) and that of upconverted PL (right y-axis), normalized to a bilayer device, as a function of the thickness of the AlQ_3 spacer. Inset: photograph of an interference-enhanced device with the λ = 980 nm pump light incident at a shallow angle. Adapted from Ref. [47].

CONCLUSIONS AND OUTLOOK

NC-sensitized upconversion has the potential to revolutionize low-cost sub-bandgap sensitization of silicon-based devices, with applications ranging from improved photovoltaics to infrared imaging. However, there are currently several major hurdles which must be overcome.

1) The infrared absorption of solid-state upconverting devices must be greatly increased. As mentioned earlier, current devices are based on single monolayers of PbS NCs and absorb well under 1% of the incident infrared photons. Preliminary results show that it is not trivial to boost the upconversion emission by simply increasing the thickness of the NC layer, likely due to the short exciton diffusion length, low PLQY of the PbS NC films, and back transfer of the singlets created by TTA in the organic semiconductor. As a result, other approaches to boosting the infrared absorption will need to be explored, where the NCs are not employed as the absorbing

layer, but only function as a spin mixer after accepting excitons from the absorber. Upconverting lanthanide nanoparticles (UCNPs) have shown great enhancement in their efficiency by using organic dyes as infrared sensitizing ligands: Zou *et al*. reported over three orders of magnitude increase in the upconversion efficiency of UCNPs when using IR 806 as a molecular antenna.[16] However, there is the risk of back transfer of a triplet exciton to the absorber when NCs are used as the sensitizer.

Besides infrared sensitization of the PbS NCs via energy transfer from high-PLQY infrared light-harvesting antennas (*e.g*. emissive bulk semiconductors or organic dyes), optical designs such as photonic crystals, waveguides, plasmonics, and luminescent solar concentrators could be utilized to concentrate incident light and/or increase its pathlength for higher absorption.

2) The strong preference for crystallization in polyacene upconverters poses an additional hurdle for the stability and performance of such devices. Due to the high molecular mobility of the polyacenes on the NC layer, the annihilator rapidly crystallizes within several days and renders the upconverting device ineffective. Effort will need to be placed on achieving long-lived, stable upconversion devices by reducing the mobility of the upconverting molecules.

3) Most TTA-based upconversion systems that upconvert infrared light utilize rubrene as the annihilator. With a triplet energy of 1.14 eV,[49] the energy of the NC sensitizers has to be above ~1.1 eV. Since silicon has a bandgap of 1.1 eV, upconversion devices using rubrene as the annihilator would not be efficient at sensitizing silicon for sub-bandgap photons. Instead, it is necessary to explore annihilators with triplet energies lower than that of rubrene.

In conclusion, NC-sensitized NIR-to-visible upconversion is an example of a hybrid inorganic/organic system with advantages unrealized by pure organic or inorganic systems. Future improvements in optical absorption, stabilizing the hybrid interface in solid-state, and red-shifting further into the infrared could enable the technology to penetrate imaging and photovoltaic applications.

CONFLICTS OF INTEREST

The authors declare no conflicts of interest.

ACKNOWLEDGMENTS

This work was primarily supported as part of the Center for Excitonics, an Energy Frontier Research Center funded by the US Department of Energy, Office of Science, Office of Basic Energy Sciences under Award Number DE-SC0001088 (MIT).

REFERENCES

1 W. Shockley and H. J. Queisser, *J. Appl. Phys.*, 1961, **32**, 510–519.
2 T. Trupke, M. A. Green and P. Würfel, *J. Appl. Phys.*, 2002, **92**, 4117–4122.
3 J. P. Mailoa, A. J. Akey, C. B. Simmons, D. Hutchinson, J. Mathews, J. T. Sullivan, D. Recht, M. T. Winkler, J. S. Williams, J. M. Warrender, P. D. Persans, M. J. Aziz and T. Buonassisi, *Nat. Commun.*, 2014, **5**, 3011.
4 S. D. Stranks, G. E. Eperon, G. Grancini, C. Menelaou, M. J. P. Alcocer, T. Leijtens, L. M. Herz, A. Petrozza and H. J. Snaith, *Science*, 2013, **342**, 341–344.
5 J. R. Poindexter, R. L. Z. Hoye, L. Nienhaus, R. C. Kurchin, A. E. Morishige, E. E. Looney, A. Osherov, J.-P. Correa-Baena, B. Lai, V. Bulović, V. Stevanović, M. G. Bawendi and T. Buonassisi, *ACS Nano*, 2017, **11**, 7101–7109.
6 G. E. Eperon, S. D. Stranks, C. Menelaou, M. B. Johnston, L. M. Herz and H. J. Snaith, *Energy Environ. Sci.*, 2014, **7**, 982–988.
7 A. Sharenko and M. F. Toney, *J. Am. Chem. Soc.*, 2016, **138**, 463–470.
8 M. Alkahtani, Y. Chen, J. J. Pedraza, J. M. González, D. Y. Parkinson, P. R. Hemmer and H. Liang, *Opt. Express*, 2017, **25**, 1030–1039.
9 J. Zhou, Q. Liu, W. Feng, Y. Sun and F. Li, *Chem. Rev.*, 2015, **115**, 395–465.
10 F. Wang, D. Banerjee, Y. Liu, X. Chen and X. Liu, *Analyst*, 2010, **135**, 1839–1854.
11 B. Zhu, B. Qian, Y. Liu, C. Xu, C. Liu, Q. Chen, J. Zhou, X. Liu and J. Qiu, *NPG Asia Mater.*, 2017, **9**, e394.
12 R. Deng, F. Qin, R. Chen, W. Huang, M. Hong and X. Liu, *Nat. Nanotechnol.*, 2015, **10**, 237.
13 Q. Tian, W. Yao, W. Wu, J. Liu, Z. Wu, L. Liu, Z. Dai and C. Jiang, *ACS Sustain. Chem. Eng.*, 2017, **5**, 10889–10899.
14 J.-H. Kim and J.-H. Kim, *J. Am. Chem. Soc.*, 2012, **134**, 17478–17481.
15 P. A. Franken, A. E. Hill, C. W. Peters and G. Weinreich, *Phys. Rev. Lett.*, 1961, **7**, 118–119.
16 W. Zou, C. Visser, J. A. Maduro, M. S. Pshenichnikov and J. C. Hummelen, *Nat. Photonics*, 2012, **6**, 560–564.
17 X. Chen, W. Xu, H. Song, C. Chen, H. Xia, Y. Zhu, D. Zhou, S. Cui, Q. Dai and J. Zhang, *ACS Appl. Mater. Interfaces*, 2016, **8**, 9071–9079.
18 F. Auzel, *Chem. Rev.*, 2004, **104**, 139–174.
19 J.-C. G. Bünzli and C. Piguet, *Chem. Soc. Rev.*, 2005, **34**, 1048–1077.
20 T. N. Singh-Rachford and F. N. Castellano, *Coord. Chem. Rev.*, 2010, **254**, 2560–2573.
21 M. Wu, D. N. Congreve, M. W. B. Wilson, J. Jean, N. Geva, M. Welborn, T. Van Voorhis, V. Bulović, M. G. Bawendi and M. A. Baldo, *Nat. Photonics*, 2016, **10**, 31–34.
22 M. Mahboub, Z. Huang and M. L. Tang, *Nano Lett.*, 2016, **16**, 7169–7175.
23 Z. Huang, X. Li, M. Mahboub, K. M. Hanson, V. M. Nichols, H. Le, M. L. Tang and C. J. Bardeen, *Nano Lett.*, 2015, **15**, 5552–5557.
24 T. F. Schulze and T. W. Schmidt, *Energy Environ. Sci.*, 2014, **8**, 103–125.
25 A. Monguzzi, R. Tubino and F. Meinardi, *J. Phys. Chem. A*, 2009, **113**, 1171–1174.
26 G. D. Scholes and G. Rumbles, *Nat. Mater.*, 2006, **5**, 683–696.

27 S. Amemori, Y. Sasaki, N. Yanai and N. Kimizuka, *J. Am. Chem. Soc.*, 2016, **138**, 8702–8705.
28 J. Kim, C. Y. Wong and G. D. Scholes, *Acc. Chem. Res.*, 2009, **42**, 1037–1046.
29 D. Y. Kondakov, T. D. Pawlik, T. K. Hatwar and J. P. Spindler, *J. Appl. Phys.*, 2009, **106**, 124510.
30 D. L. Dexter, *J. Chem. Phys.*, 1953, **21**, 836–850.
31 G. D. Scholes, *Ann. Rev. Phys. Chem.*, 2003, **54**, 57–87.
32 L. Nienhaus, M. Wu, N. Geva, J. J. Shepherd, M. W. B. Wilson, V. Bulović, T. Van Voorhis, M. A. Baldo and M. G. Bawendi, *ACS Nano*, 2017, **11**, 7848–7857.
33 N. J. Thompson, M. W. B. Wilson, D. N. Congreve, P. R. Brown, J. M. Scherer, T. S. Bischof, M. Wu, N. Geva, M. Welborn, T. V. Voorhis, V. Bulović, M. G. Bawendi and M. A. Baldo, *Nat. Mater.*, 2014, **13**, 1039–1043.
34 D. V. Talapin and C. B. Murray, *Science*, 2005, **310**, 86–89.
35 M. Tabachnyk, B. Ehrler, S. Gélinas, M. L. Böhm, B. J. Walker, K. P. Musselman, N. C. Greenham, R. H. Friend and A. Rao, *Nat. Mater.*, 2014, **13**, 1033.
36 D. a. G. Bruggeman, *Ann. Phys.*, 1935, **416**, 636–664.
37 Z. Huang, Z. Xu, M. Mahboub, X. Li, J. W. Taylor, W. H. Harman, T. Lian and M. L. Tang, *Angew. Chem.*, 2017, **129**, 16810–16814.
38 Z. Huang and M. L. Tang, *J. Am. Chem. Soc.*, 2017, **139**, 9412–9418.
39 S. Garakyaraghi, C. Mongin, D. B. Granger, J. E. Anthony and F. N. Castellano, *J. Phys. Chem. Lett.*, 2017, **8**, 1458–1463.
40 N. Geva, J. J. Shepherd, L. Nienhaus, M. G. Bawendi and T. Van Voorhis, *arXiv:1706.00844 [physics.chem-ph]*, 2018, arXiv.org e-Print archive. https://arxiv.org/abs/1706.00844 (accessed Jan 29, 2018).
41 M. Green, *J. Mater. Chem.*, 2010, **20**, 5797–5809.
42 A. Maliakal, K. Raghavachari, H. Katz, E. Chandross and T. Siegrist, *Chem. Mater.*, 2004, **16**, 4980–4986.
43 Z. Huang, D. E. Simpson, M. Mahboub, X. Li and M. L. Tang, *Chem. Sci.*, 2016, **7**, 4101–4104.
44 J. M. Pietryga, D. J. Werder, D. J. Williams, J. L. Casson, R. D. Schaller, V. I. Klimov and J. A. Hollingsworth, *J. Am. Chem. Soc.*, 2008, **130**, 4879–4885.
45 M. Nasilowski, L. Nienhaus, S. N. Bertram and M. G. Bawendi, *Chem. Commun.*, 2017, **53**, 869–872.
46 I. Moreels, K. Lambert, D. Smeets, D. De Muynck, T. Nollet, J. C. Martins, F. Vanhaecke, A. Vantomme, C. Delerue, G. Allan and Z. Hens, *ACS Nano*, 2009, **3**, 3023–3030.
47 M. Wu, J. Jean, V. Bulović and M. A. Baldo, *Appl. Phys. Lett.*, 2017, **110**, 211101.
48 J.-C. Boyer and F. C. J. M. van Veggel, *Nanoscale*, 2010, **2**, 1417–1419.
49 W. G. Herkstroeter and P. B. Merkel, *J. Photochem.*, 1981, **16**, 331–341.